Equal Rights for Activators – Ytterbium to Terbium Cooperative Sensitization in Molecular Upconversion

Federico Pini, Richard C. Knighton, Lohona K. Soro, Loïc J. Charbonnière, Marta M. Natile,* and Niko Hildebrandt*

Molecular scaffolds are ideal for investigating upconversion (UC) at the highest spatial resolution and to create precisely controllable luminescent materials. Such control may be the key to overcoming the limitations of brightness and reproducibility found in UC micro- and nanoparticles. Cooperative UC can significantly increase luminescence brightness and bulk studies showed that highest efficiencies can be obtained by sensitizer-to-activator ion ratios ≥ 2, that is, via high probabilities of sensitizing the emitting lanthanide ion. Using nonanuclear molecular complexes, the authors demonstrate both experimentally and theoretically that interion distances are more relevant and that the highest UC efficiencies are actually attained for sensitizer-to-activator ion ratios around 1. By modeling accretive and cooperative sensitization UC, energy migration, and fitting experimental data, it is revealed that cooperative sensitization is predominant for the determination of UC luminescence intensities, whereas energy migration defines UC luminescence kinetics. The implementation of interion distances and different energy transfer mechanisms into advanced modeling of experimental UC data will be paramount for designing brighter and better UC materials.

1. Introduction

Upconversion (UC) of near-infrared (NIR) to visible photons in solids,[1,2] submicron particles (UC phosphors),[3,4] and nanoparticles (UC nanoparticles),[5–7] and in solution (triplet–triplet annihilation)[8,9] has been studied for many years and applied to photovoltaics, photocatalysis, bioanalysis, or theranostics.[10–14] Despite the advances in material design and optimization, UC micro and nanoparticles have arguably reached the limits of brightness and reproducibility and new concepts are necessary for further improvements. Intramolecular UC within discrete molecular compounds is a recent approach that has the potential to advance UC performance via precise molecular building blocks.[15–20] However, molecular UC is a very young research field that still requires a lot of fundamental investigations and understanding before experimental

F. Pini, M. M. Natile
Istituto di Chimica della Materia Condensata e Tecnologie per l'Energia (ICMATE)
Consiglio Nazionale delle Ricerche (CNR)
Padova 35131, Italy
E-mail: martamaria.natile@unipd.it
F. Pini, M. M. Natile
Dipartimento di Scienze Chimiche
Università di Padova
Padova 35131, Italy
F. Pini, N. Hildebrandt
Laboratoire COBRA
CNRS
INSA Rouen
Université de Rouen Normandie
Normandie Université
Mont-Saint-Aignan 76821, France
E-mail: hildebrandt@mcmaster.ca

R. C. Knighton, L. K. Soro, L. J. Charbonnière
Equipe de Synthèse pour L'Analyse (SynPA)
Institut Pluridisciplinaire Hubert Curien (IPHC)
UMR 7178
CNRS
ECPM
Université de Strasbourg
25 rue Becquerel, Strasbourg 67087, France

R. C. Knighton
School of Chemistry
University of Southampton
Southampton SO17 1BJ, UK

N. Hildebrandt
Department of Chemistry
Seoul National University
Seoul 08826, South Korea

N. Hildebrandt
Department of Engineering Physics
McMaster University
Hamilton, ON L8S4L7, Canada

breakthroughs concerning brightness improvement can become reality. In the status quo, molecular complexes have shown to be extremely sensitive to deactivation processes, such as vibrational losses to the ligand or solvent molecule overtones, which result in significantly lower UC efficiencies compared to UC phosphors or UC nanoparticles.[21–23] Different concepts, such as sensitization of the Er activator via an energy transfer UC (ETU) mechanism from organic dye antennas,[24–26] cooperative luminescence from numerous Yb ions,[27] or cooperative sensitization UC (CSU) via two sensitizers to brighter Tb or Ru activators,[20,28,29] have been developed with the aim to increase molecular UC luminescence (UCL) signals. Although experimental advances have resulted in more efficient molecular UC complexes, synthetic approaches alone will not be sufficient to accomplish brightness levels that can compete with UC nanoparticles. In nano, micro, and bulk crystalline materials, theoretical understanding and modeling of the different sensitization and deactivation processes between sensitizers, activators, and their environment have been studied in detail for ETU[30–32] and CSU[33,34] processes, and that knowledge has advanced UC nanoparticles to widely applied luminescent materials. However, the exact same principles that were established for those crystalline materials are not applicable to molecular UC complexes and thus, new models are paramount to better understand and improve molecular UC. This is especially true for the relatively young research field of molecular UC, for which UCL quantum yields accomplished so far span five orders of magnitude from 10^{-9} to 10^{-4} (Figure S1, Supporting Information). A recent study showed that co-crystallization of molecular UC complexes can lead to UC quantum yields that are even close to those of UCNPs.[35] To accelerate the advancement of UC molecules to actual applications and not rely on decades of optimization, as previously done for UCNPs, the implementation of advanced modeling is clearly a key solution.

2. Results and Discussion

2.1. Statistical Distribution of Lanthanide Ions in Nonanuclear Complexes

Recently, we reported the synthesis and characterization of a combinatorial library of hetero-nonanuclear lanthanide complexes ($[Ln_9(acac)_{16}(OH)_{10}]OH$), including a detailed experimental investigation of their UC properties in solution.[28] The complexes' stoichiometries covered the range of all possible combinations of trivalent Yb ions as sensitizers (energy donors), Tb ions as activators (energy acceptors), and Y ions as spectroscopically silent surrogates, such that the final stoichiometry was $Tb_xYb_yY_z$ (with x, y, and z integer values and $x + y + z = 9$). Whereas some of the studied UC properties met the expectations based on the current state-of-the-art (e.g., excitation power dependence, UCL lifetime, effect of deuterium substitution in the ligands), the stoichiometry for the brightest complex was unexpected. Because CSU is a sensitized process (from at least two Yb sensitizers to one Tb activator), it would have been expected that higher ratios of Yb-per-Tb result in higher UC efficiency.[2,36] However, the most efficient UCL was found for Tb/Yb (i.e., x/y) ratios close to unity
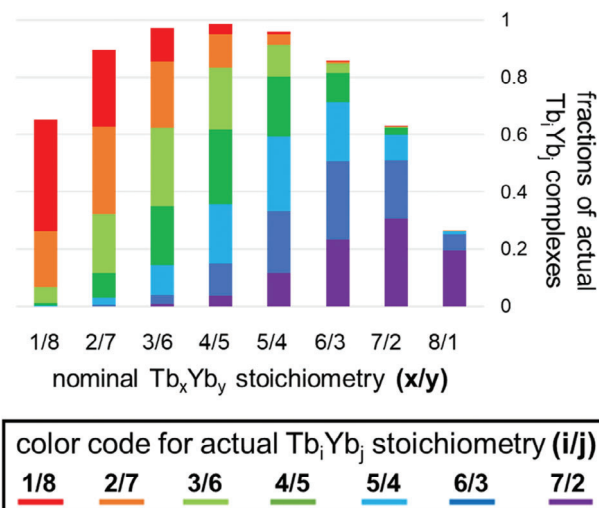
Figure 1. Fractions of actually formed Tb_iYb_j nonanuclear complexes as a function of nominal Tb_xYb_y mixtures (x/y presents the Tb-to-Yb concentration ratio).

(4/5 or 5/4),[28] a phenomenon also observed for other molecular UCL devices.[16,37]

Considering a statistical distribution, the nominal stoichiometry (of the used lanthanide ion concentrations in the fabrication of the complexes) does not equal the actual stoichiometry (within the actually formed complexes), which explains why in our experimental study even for nominal Tb_8Yb_1 complexes significant UCL was observed.[28] Considering a statistical distribution of the Ln atoms in the complex, the actually formed complexes contained more than 26% of species with two or more Yb ions because the probability of complexes with an actual stoichiometry Tb_iYb_j formed from a nominal Tb_xYb_y composition is as follows.

$$P_{i,j} = \frac{n!}{i!j!}\left(\frac{x}{n}\right)^i\left(\frac{y}{n}\right)^j \tag{1}$$

where n stands for the number of Ln ions in the complex, with $n = 9$ in our case of nonanuclear complexes. Whereas this probability distribution also shows that the maximum fraction of CSU complexes is formed for x/y ratios between ≈3/6 and 6/3 (**Figure 1**), it does not explain why the most efficient UCL was found for x/y ratios of 5/4 and 4/5.

2.2. CSU Isomers and Interionic Distances

To understand the difference between the expected and experimentally obtained UCL, the complete distribution of Tb and Yb ions and their interionic distances, which define the strengths of energy transfer interactions between the ions, must be accounted for, and the overall CSU must be calculated from the entire set of actual complex conformations. As mentioned above, a nominal stoichiometry (input concentrations for the synthesis of complexes) of Tb_xYb_y will produce a close-to statistical distribution of possible complexes with real or actual stoichiometry of Tb_iYb_j. Each of these actual complexes will then result in a family of configurations (isomers), in which the Tb and Yb ions can randomly
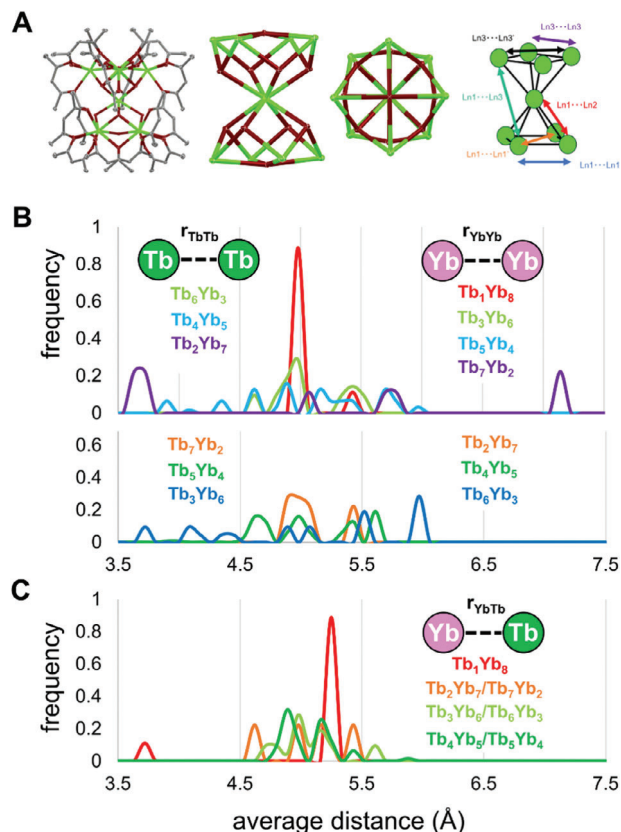
Figure 2. A) Single-crystal X-ray structure of a $[Tb_xYb_y(acac)(OH)_9(O)_1]$ complex ($x = 4.5$, $y = 4.5$), from left to right: Full structure, nonanuclear Ln_9 core, top-down view of Ln_9 core (H-atoms and solvent molecules omitted for clarity, ellipsoids plotted at the 50% probability level), schematic depiction of the nonanuclear core including atom numbering for specific interion distances (CCDC no. 2333808). Frequency distribution of the average B) Yb-to-Yb and Tb-to-Tb and C) Yb-to-Tb distances (r) calculated for all isomer configurations of a given Tb_iYb_j complex. Tb_8Yb_1, Tb_9Yb_0, and Tb_0Yb_9 are not included because at least 2 Yb ions and 1 Tb ion are necessary for CSU.

oxygens from one bidentate and two bridging acetylacetonate ligands. The cluster displays local four-fold symmetry in the solid state, meaning only one top and bottom vertex are crystallographically unique, exhibiting perfect squares on the top and bottom faces (90.0000 ± 0.0013° and 90.00000 ± 0.00018°). The pertinent interatomic distances (Figure 2A, and Figure S4, Supporting Information) were determined to be 3.5931 ± 0.0003 Å (Ln1–Ln1 and Ln3–Ln3) for the square edges and 5.0317 ± 0.0004 Å (Ln1–Ln1') or 5.0814 ± 0.0004 Å (Ln3–Ln3') for the base diagonals. The largest intracluster ion distance was 7.1385 ± 0.0003 Å (Ln1–Ln3'). Comparison of the single-crystal X-ray diffraction metrics of the heterometallic $Tb_{4.5}Yb_{4.5}$ mixture with a previously reported Tb_9 homolog revealed only a small covariance between the two (Table S1, Supporting Information).[38] Overall, the intermetallic distances were elongated in the homometallic cluster, due to the larger radius of Tb^{III} versus Yb^{III}, showing deviations typically below 1% between the two structures. This demonstrates that changes in interion distances are negligible when considering the Tb–Tb, Tb–Yb, and Yb–Yb distances in co-doped clusters. With the exactly determined positions of the lanthanides in the clusters, the variable that determines the figure of merit for CSU is the ion-to-ion distance distribution for the different isomer configurations. Using a purposely developed Python code (Supporting Information), we simulated all the $N_{i,j}$ isomer configurations for each Tb_iYb_j complex to calculate the final distribution of Yb-to-Yb, Tb-to-Tb, and Yb-to-Tb average distances (Figure 2).

The Yb-to-Yb average distance distribution becomes narrower with increasing amounts of Yb. For example, for Tb_1Yb_8 (red curve in Figure 2B) all average Yb–Yb distances are within a 5 to 5.5 Å range, for Tb_4Yb_5 (dark green curve in Figure 2B) the distribution broadens to a range between 4 and 6 Å, and for Tb_7Yb_2 (purple curve in Figure 2B) the Yb–Yb distances are broadly distributed between ≈3.5 and 7.3 Å. For Tb-to-Tb distances, the distributions are a mirror of the Yb/Yb configurations with an inverted trend of narrowing with increasing amounts of Tb. For Tb-to-Yb distances (Figure 2C), the distributions are narrower because they are the same for Tb_iYb_j and Tb_jYb_i. Notably, the distribution becomes more compact for the complexes with Tb-to-Yb ratios close to 1. The only complex that does not have a symmetrical analog is Tb_1Yb_8 (because Tb_8Yb_1 cannot produce CSU). For this complex, the distance distribution provides only two possible distances, for which 5.25 Å corresponds to the Tb ion in one of the two bases of the bipyramid and 3.72 Å corresponds to the Tb ion on the vertex of the two pyramids. This assignment is also confirmed by the probability of the two distances, with the shorter one being eight times less probable than the longer one.

2.3. Different Mechanisms of CSU

To calculate the actual UCL contributions, the statistical distribution of actual complexes and the interion distance distributions within all possible complex configurations need to be combined with CSU probability laws. Lanthanide energy transfer probabilities have been investigated in bulk systems (e.g., solid-state laser materials and solutions), microsystems (e.g., powders and microparticles), and nanosystems (e.g., UC and other NPs) for many years.[39–42] Despite the development of several sophisticated

occupy any of the nine different possible sites of the nonanuclear complex. Disregarding the symmetry elements of the complex this leads to 9 Tb_1Yb_8, 36 Tb_2Yb_7, 84 Tb_3Yb_6, 126 Tb_4Yb_5, 126 Tb_5Yb_4, 84 Tb_6Yb_3, and 36 Tb_7Yb_2 possible CSU isomers (Figure S2, Supporting Information). To determine the interion distances within the different isomer configurations, we performed single-crystal X-ray crystallography (Supporting Information). Crystals were obtained from a solution of concentrated MeOH cooled to −18 °C and the data were collected at 100 ± 2 K. In contrast to the complex in the solution-state ($[Ln_9(acac)_{16}(OH)_{10}]OH$), solid-state crystals were obtained as $[Tb_xYb_y(acac)_{16}(OH)_9(O)_1]$ complexes ($x = 4.5$, $y = 4.5$). The compound crystallized in the $P4/n$ space group and was isostructural and isomorphous with previously reported Ln_9 clusters.[28] The structure (**Figure 2A**) displays a nonanuclear core, consisting of two square-based pyramids that share the central Ln vertex, such that the overall structure is that of an hourglass arrangement, with the top and bottom half rotated by ≈45°. The Ln center is octacoordinated, ligated by eight μ_3-OH ligands. The remaining eight atoms are eight coordinated, connected by two μ_3-OH, one μ_4-O/OH bridge, and five

**ADVANCED
SCIENCE NEWS**

www.advancedsciencenews.com

**ADVANCED
OPTICAL
MATERIALS**

www.advopticalmat.de

models for understanding energy transfer processes,[43–45] several of their bulk-system approximations (e.g., large number of ions and isotropy of the system) are not applicable to molecular systems. Although the fundamental ET interactions, that is, electrostatic multipolar interaction (Förster-like)[46,47] and exchange interaction through wavefunction overlap (Dexter-like),[48,49] apply to any system from the molecular to the bulk scale, the distinction between these two mechanisms is difficult from experimental data of complex systems, in particular, for cooperative processes. For this reason, we focused our analysis on multipolar interaction cooperative ET probabilities.

Kushida and Auzel proposed two concurring mechanisms of CSU,[1,47] which can be defined as accretive and cooperative, in analogy to downconversion (i.e., quantum cutting). Both mechanisms require polarization induced by a virtual state of opposite parity. In the accretive one (P_{Ac}, Equation (2)) the virtual state is localized on one of the Yb ions, thus the excitation must first pass from another Yb to the virtual state, and then, when this state is charged, to the Tb acceptor. For this reason, the accretive mechanism depends on both Yb–Yb and Yb–Tb distances. On the other hand, the cooperative mechanism probability (P_{Co}, Equation (3)) depends only on Yb–Tb distances because the virtual state is located on the acceptor (Tb), which gets charged by ET from two Yb, disregarding the mutual position of the two sensitizers, and then transfer the energy to the Tb ion.[50] The probability law was first derived by Kushida for a trimeric system composed of two sensitizers (Yb) and one activator (Tb). Here we adapted the approach to multimeric systems,[47] similar to what was first proposed by Inokuti and Hirayama and later adapted algorithmically by Vergeer et al. for quantum cutting in nanomaterials.[45,50] As outlined in our previous work,[28] the increase of the nominal fraction of Yb in the complexes led to a decrease in the UCL lifetime (Figure S3A, Supporting Information), which suggests the presence of energy migration (EM) via Yb ions, similarly to what has been observed in nanomaterials.[51,52] Thus, we also included an EM probability (P_{EM}, Equation (4)) in our theoretical model. EM describes the transfer of energy from an excited-state Yb ion to a ground-state Yb ion in close proximity. This energy migration can lead to very beneficial effects in nano- and micromaterials because it allows excitons to migrate over long distances to reach the emitting activator ions. On the other hand, it can also have detrimental effects because it can trap the exciton in quenchable (dark) states and facilitate migration to the particle surface, which is heavily exposed to the UCL-quenching environment.[53] For the small dimensions of molecular UC complexes in diluted solutions, migration over long distances is not possible. Therefore, energy migration can only result in detrimental effects that facilitate the loss of excitons through the deactivation of Yb ions. EM via Tb ions is in principle also possible and was included in our initial model. However, the experimental data could be adequately fit without the Tb-Tb interaction term and thus, to avoid an over-parametrization of the problem, we decided to omit Tb–Tb EM. A probable explanation of the minor influence of Tb–Tb EM compared to Yb–Yb EM is the larger Tb energy gap, which results in a significantly lower quenching probability.

$$P_{Ac} = A_{AC} \sum_{a}^{N_{Yb}} \sum_{b \neq a}^{N_{Yb}} \sum_{c}^{N_{Tb}} \left(\frac{1}{\left(r_{Yb_a Yb_b} r_{Yb_a Tb_c}\right)^{2p}} + \frac{1}{\left(r_{Yb_a Yb_b} r_{Yb_b Tb_c}\right)^{2p}} \right) \quad (2)$$

$$P_{Co} = A_{Co} \sum_{a}^{N_{Yb}} \sum_{c}^{N_{Tb}} \frac{1}{\left(r_{Yb_a Tb_c}\right)^{4p}} \quad (3)$$

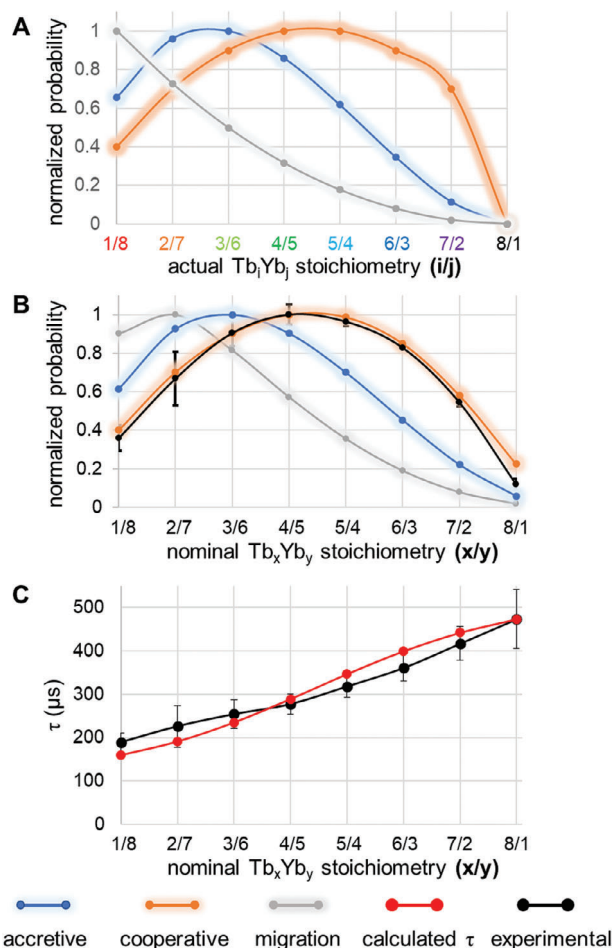$$P_{EM} = A_{EM} \sum_{a}^{N_{Yb}} \sum_{b \neq a}^{N_{Yb}} \frac{1}{\left(r_{Yb_a Yb_b}\right)^{2p}} \quad (4)$$

The accretive probability (Equation (2)) contains a triple summation over the indices of Yb (a and b, which must be different) and Tb ions (c), which describe the positions in which the ions are placed inside the complex structure. The cooperative probability (Equation (3)) depends solely on Yb-to-Tb distances, whereas the EM probability (Equation (4)) depends only on Yb-to-Yb distances and would present a negative contribution to UCL. The distances (r) are those between the different ions in the different positions (a, b, and c) within the complex structures. The parameter p determines the type of interaction between ions, which can be 3, 4, etc. for dipole–dipole, dipole–quadrupole, etc. Trials with different values of p led to minor differences in the resulting probabilities and thus, we used the dipole-dipole interaction with p = 3. The parameters A_{Ac}, A_{Co}, and A_{EM} present the probability amplitudes, which have units Å^{12} for cooperative and accretive mechanisms and Å^6 for energy migration, in order to obtain dimensionless probabilities.

Equations (2–4) were used to calculate the different expected probabilities for each configuration within each actual stoichiometry. The average of those distinct probabilities provided the overall probability of accretive CSU, cooperative CSU, and EM for each actual nonanuclear Tb$_i$Yb$_j$ complex (**Figure** 3A). As expected, the EM probability (grey line in Figure 3A) increased with increasing fractions of Yb and showed a difference of ≈100% between Tb$_7$Yb$_2$ and Tb$_1$Yb$_8$. Cooperative CSU (orange line in Figure 3A) as a function of i/j stoichiometry appeared as a symmetric bell shape, mimicking the Yb-to-Tb distance distribution, and showing maximum probabilities for Tb$_4$Yb$_5$ and Tb$_5$Yb$_4$ complexes. These results suggest that the narrower the average interion distance distribution (Figure 2) the higher the CSU probability. Accretive CSU (blue line in Figure 3A) contains both Yb-to-Yb and Tb-to-Yb contributions, which resulted in a probability function with an unsymmetric bell shape that was shifted to Yb-richer complexes with a maximum for Tb$_3$Yb$_6$. Importantly, the CSU probabilities for these actual complexes differ from the expectation that more Yb sensitizers would lead to stronger CSU. This result is strongly connected to the interion distances within the complexes and is therefore dependent on the complex composition and not only on the fraction of sensitizers and activators.

2.4. Modeling of Experimental Results

To model the actual experimental results, the probabilities of each phenomenon for the nominal complex stoichiometries Tb$_x$Yb$_y$ are required. These were obtained by multiplying the probability of accretive CSU, cooperative CSU, and EM (Figure 3A) by the probability of having a certain actual complex (Tb$_i$Yb$_j$) given a nominal stoichiometry (Equation (1) and Figure 1). The results (Figure 3B) show that maximum probabilities were obtained with Tb$_2$Yb$_7$ (i.e., x/y = 2/7) for EM, with Tb$_4$Yb$_5$ (i.e., x/y = 4/5) for cooperative CSU, and with Tb$_3$Yb$_6$ (i.e., x/y = 3/6) for accretive

**ADVANCED
SCIENCE NEWS**

www.advancedsciencenews.com

**ADVANCED
OPTICAL
MATERIALS**

www.advopticalmat.de

Figure 3. Normalized probabilities of accretive CSU (blue), cooperative CSU (orange), and EM (gray) for A) each actual Tb_iYb_j complex and B) each nominal Tb_xYb_y complex. Same colors are shown for the respective probabilities in (B), while the black curve in (B) shows the experimental CSU obtained from UCL decay curves (Figure S3, Supporting Information). C) Normalized average UCL lifetimes for each nominal Tb_xYb_y complex: calculated (red line) and experimental (black curve). The black curve was derived from the biexponential fitting of the UCL decay curves (Figure S3, Supporting Information). The error bars in (B,C) present SDs from measuring three independently prepared samples.

CSU. Notably, the cooperative mechanism for CSU (orange curve in Figure 3B) mimics almost perfectly the experimental CSU data (black curve in Figure 3B), which represent UCL intensities calculated from UCL kinetics with long (60 μs) excitation pulses. This result shows that the accretive mechanism, as pointed out in quantum cutting studies,[50] and EM are not required to explain the experimental CSU intensity data for the nonanuclear molecular UC complexes. Nevertheless, both mechanisms may be important to describe the UCL intensities of other UC complexes. In that case, the sum of all three mechanisms can be fit into the experimental data to calculate the contribution of each to the overall UCL intensity.

Interestingly, our model can also predict ETU probabilities for molecular UC complexes. Again, nonanuclear complexes with equal amounts of sensitizers and activators were identified as the best system (i.e., x/y and i/j ratios of 4/5 and 5/4 – Equa-

tion (S1) and Figure S5, Supporting Information), which is in strong contrast to the optimum sensitizer-activator ratios in UC phosphors or nanoparticles that are usually around 9 (18% Yb and 2% Er).[54,55] Unfortunately, sufficiently bright UCL could not be accomplished with ETU in our nonanuclear complexes because the common ETU activator ions, such as Er or Tm, are much more prone to non radiative deactivation due to their energy level structure. Nevertheless, the theoretical prediction of the highest ETU probability in nonanuclear complexes via sensitizer-activator ratios around unity shows that unprecedented and possibly brighter materials may become accessible via molecular UC. If ETU complexes including more than three ions can be developed in the future, it would be highly interesting to apply our model and verify this theoretical assumption.

2.5. UCL Lifetimes and Energy Migration

Although EM was not required to explain the experimental CSU intensities, it can be very useful to model the CSU lifetimes, since these showed a clear dependence on the Yb content (black line in Figure 3C). The expression of the calculated average CSU lifetime for each nominal (x/y) composition ($\tau_{x,y}$, Equation (5)) can be written as the weighted average of the lifetimes of the actual (i/j) complexes ($\tau_{i,j}$), where the weighting factor ($\alpha_{i,j}$) describes the probability ($P_{i,j}$) to obtain an actual composition given a nominal one. The complex stoichiometry-dependent CSU lifetime is determined via the population and depopulation of Yb ion energy levels (Supporting Information). Therefore, the CSU lifetime of each actual stoichiometry can be expressed as the sum of all processes leading to the deactivation of Yb ions for each complex, that is, the deactivation of the isolated ion (k_0) and EM.

$$\tau_{x,y} = \sum_{(i,j)} \alpha_{i,j}\tau_{i,j} = \frac{\sum_{(i,j)} P_{i,j}\tau_{i,j}}{\sum_{(i,j)} P_{i,j}} \tag{5}$$

$$\tau_{i,j} = \frac{1}{k_0 + EM} = \frac{\tau_0}{\left(1 + P_{EM}^{i/j}\right)} \tag{6}$$

Using Equations (5) and (6) we were able to compare the experimental average lifetimes for each nominal stoichiometry x/y (Figure S2, Supporting Information) with the calculated ones. When fitting the experimental UCL lifetimes (black curve in Figure 3C) with Equation (5), $P_{i,j}$ was fixed and determined from statistical considerations (Equation (1)). $P_{EM}^{i/j}$ (the energy migration probability for a given actual composition, Equation (4)) was determined by the distance distribution and by the amplitude parameter A_{EM}. Thus, the only fit parameters to obtain the calculated lifetimes were τ_0 and A_{EM}. The optimal values for these parameters were $\tau_0 = 475$ μs and $A_{EM} = 2630$ Å⁶, which reproduced the experimental average lifetime with very good accuracy (red curve, Figure 3C) and confirmed the initial hypothesis of an important contribution of EM to the CSU lifetimes. The finding that EM did not play a role in the determination of CSU intensities but significantly contributed to the CSU lifetimes may seem counterintuitive. However, UCL is dependent on many energy levels, energetic transitions, and interactions between different

**ADVANCED
SCIENCE NEWS**

www.advancedsciencenews.com

**ADVANCED
OPTICAL
MATERIALS**

www.advopticalmat.de

ions, which can result in a dominant contribution of the cooperative mechanism for CSU intensities, whereas the decay kinetics from the final excited state may still be strongly influenced by EM. Another explanation would be an equilibrium between the accretive mechanism (positive contribution for CSU intensities) and EM (negative contribution for CSU intensities), where one contribution compensates the other (because of their similar dependence on nominal stoichiometry – Figure 3B), such that only the cooperative mechanism determines the overall CSU intensity.

Including the luminescence lifetime of the Yb sensitizers or the rise time of the Tb UCL in the analysis and modeling could in principle provide an even better understanding of the entire molecular UC process. Yb emission can be observed upon both ligand and Tb excitation via downshifting.[28] For our complexes, Yb downshifting luminescence lifetimes were 15 µs for Yb_9, 17 µs for Tb_1Yb_8, 18 µs for Tb_3Yb_6, and 20 µs for Tb_4Yb_5, and Tb UCL lifetimes were 189 µs for Tb_1Yb_8, 254 µs for Tb_3Yb_6, and 277 µs for Tb_4Yb_5.[28] Due to the significantly stronger change in the UCL lifetimes, our model focused on UCL only. With the same aim of using as few parameters as possible for a simple but still accurate analytical model, we also omitted the rise time parts of the Tb UCL. However, we also developed a semi-analytical model that could fit the complete (rise and decay) UCL kinetics and also validated our simpler and more intuitive analytical approach (Supporting Information).

3. Conclusions

In conclusion, we theoretically confirmed the experimental findings that similar amounts (ratio close to 1) of sensitizers and activators result in the highest UC efficiencies in molecular CSU complexes. This result is highly important as it has been commonly assumed that large ratios of sensitizers per activator lead to high UCL efficiencies because more sensitizers should provide a higher probability of sensitizing the emitting activator ion. Because brightness is also influenced by the absorption cross-section and the quenching of the sensitizers (both increase with the number of sensitizers), the sensitizer-to-activator ratio cannot be too high either. However, ratios ≥ 2 are considered to be beneficial for UC brightness. Whereas this assumption may be true for systems with equal distances between all ions and in large upconversion ensembles (i.e., nano- or microparticles), for which energy migration over long distances is necessary to efficiently reach the final activator ion, it is not a general fact for upconversion. Using nonanuclear complexes, in which Yb sensitizers and Tb activators in Tb/Yb concentration ratios between 1/8 and 8/1 were allowed to take any possible position within the complexes, we demonstrated experimentally that ratios close to unity (i.e., 5/4 and 4/5) yielded the brightest UCL. This finding was confirmed by a theoretical model that calculated the contributions of accretive CSU, cooperative CSU, and EM based on all possible interion distances in the nonanuclear complexes. The model provided excellent concordance with the experimental data when only the cooperative mechanism was taken into account for CSU. Our results show that interion distances (and not sensitizer/activator ratios) are the most important parameter for the determination of UC efficiencies and that accretive CSU and EM played minor roles for UCL intensities

in the nonanuclear complexes. Interestingly, the model also predicted the highest UCL efficiencies for ETU-based nonanuclear complexes (e.g., Yb sensitizers and Er activators). However, due to their very low brightness, such ETU complexes could unfortunately not be investigated experimentally. Despite the predominance of cooperative CSU in UCL intensity, EM could be used to model the UCL decays with a very good fit between the model and the experimental data. Our approach of combined theoretical modeling and experimental analysis of the UCL decays provided a better understanding of the mechanisms that drive UCL intensity and decay kinetics in molecular UC and showed that interion distance is extremely important when studying UC on a molecular scale. Considering that our model can be applied to any UC system for which interion distances are known, our results are also important for reconsidering the mechanisms of UC in general and to stimulate the appreciation and careful analysis of interion distances for designing more efficient UC nanoparticles.

Supporting Information

Supporting Information is available from the Wiley Online Library or from the author.

Conflict of Interest

The authors declare no conflict of interest.

Data Availability Statement

The data that support the findings of this study are available from the corresponding author upon reasonable request.

Keywords

[1] F. Auzel, *J. Lumin.* **1990**, *45*, 341.

[2] F. Auzel, *Chem. Rev.* **2004**, *104*, 139.

[3] W. H. Wright, N. A. Mufti, N. T. Tagg, R. R. Webb, L. V. Schneider, in *High-Sensitivity Immunoassay Using a Novel Upconverting Phosphor Reporter* (Eds.: G. E. Cohn, S. A. Soper), SPIE, San Jose, CA **1997**, pp. 248-255.

[4] T. Soukka, K. Kuningas, T. Rantanen, V. Haaslahti, T. Lövgren, *J. Fluoresc.* **2005**, *15*, 513.

[5] U. Resch-Genger, H. H. Gorris, *Anal. Bioanal. Chem.* **2017**, *409*, 5855.

[6] A. Gnach, T. Lipinski, A. Bednarkiewicz, J. Rybka, J. A. Capobianco, *Chem. Soc. Rev.* **2015**, *44*, 1561.

[7] M. Haase, H. Schäfer, *Angew. Chem., Int. Ed.* **2011**, *50*, 5808.

[8] C. A. Parker, C. G. Hatchard, E. J. Bowen, *Proc. R. Soc. London, Ser. A* **1997**, *269*, 574.

[9] N. Yanai, N. Kimizuka, *Acc. Chem. Res.* **2017**, *50*, 2487.

[10] K. Kuningas, T. Rantanen, T. Ukonaho, T. Lövgren, T. Soukka, *Anal. Chem.* **2005**, *77*, 7348.

[11] G. Sun, Y. Xie, L. Sun, H. Zhang, *Nanoscale Horiz.* **2021**, *6*, 766.

[12] B. S. Richards, D. Hudry, D. Busko, A. Turshatov, I. A. Howard, *Chem. Rev.* **2021**, *121*, 9165.

[13] Y. Wang, S. Song, S. Zhang, H. Zhang, *Nano Today* **2019**, *25*, 38.

[14] G. Tessitore, G. A. Mandl, M. G. Brik, W. Park, J. A. Capobianco, *Nanoscale* **2019**, *11*, 12015.

[15] L. Aboshyan-Sorgho, C. Besnard, P. Pattison, K. R. Kittilstved, A. Aebischer, J.-C. G. Bünzli, A. Hauser, C. Piguet, *Angew. Chem., Int. Ed.* **2011**, *50*, 4108.

[16] A. M. Nonat, L. J. Charbonnière, *Coord. Chem. Rev.* **2020**, *409*, 213192.

[17] H. Bolvin, A. Fürstenberg, B. Golesorkhi, H. Nozary, I. Taarit, C. Piguet, *Acc. Chem. Res.* **2022**, *55*, 442.

[18] B. Golesorkhi, A. Fürstenberg, H. Nozary, C. Piguet, *Chem. Sci.* **2019**, *10*, 6876.

[19] B. Golesorkhi, H. Nozary, A. Fürstenberg, C. Piguet, *Mater. Horiz.* **2020**, *7*, 1279.

[20] R. C. Knighton, L. K. Soro, W. Thor, J.-M. Strub, S. Cianférani, Y. Mély, M. Lenertz, K.-L. Wong, C. Platas-Iglesias, F. Przybilla, L. J. Charbonnière, *J. Am. Chem. Soc.* **2022**, *144*, 13356.

[21] C. Doffek, N. Alzakhem, C. Bischof, J. Wahsner, T. Güden-Silber, J. Lügger, C. Platas-Iglesias, M. Seitz, *J. Am. Chem. Soc.* **2012**, *134*, 16413.

[22] Y. Feng, Z. Li, Q. Li, J. Yuan, L. Tu, L. Ning, H. Zhang, *Light: Sci. Appl.* **2021**, *10*, 105.

[23] F. Pini, L. Francés-Soriano, N. Peruffo, A. Barbon, N. Hildebrandt, M. M. Natile, *ACS Appl. Mater. Interfaces* **2022**, *14*, 11883.

[24] I. Hyppänen, S. Lahtinen, T. Ääritalo, J. Mäkelä, J. Kankare, T. Soukka, *ACS Photonics* **2014**, *1*, 394.

[25] B. Golesorkhi, S. Naseri, L. Guénée, I. Taarit, F. Alves, H. Nozary, C. Piguet, *J. Am. Chem. Soc.* **2021**, *143*, 15326.

[26] I. Taarit, F. Alves, A. Benchohra, L. Guénée, B. Golesorkhi, A. Rosspeintner, A. Fürstenberg, C. Piguet, *J. Am. Chem. Soc.* **2023**, *145*, 8621.

[27] L. K. Soro, R. C. Knighton, F. Avecilla, W. Thor, F. Przybilla, O. Jeannin, D. Esteban-Gomez, C. Platas-Iglesias, L. J. Charbonnière, *Adv. Opt. Mater.* **2023**, *11*, 2202307.

[28] R. C. Knighton, L. K. Soro, L. Francés-Soriano, A. Rodríguez-Rodríguez, G. Pilet, M. Lenertz, C. Platas-Iglesias, N. Hildebrandt, L. J. Charbonnière, *Angew. Chem., Int. Ed.* **2022**, *61*, 202113114.

[29] D. A. Gálico, M. Murugesu, *Angew. Chem., Int. Ed.* **2022**, *61*, 202204839.

[30] S. Wen, J. Zhou, K. Zheng, A. Bednarkiewicz, X. Liu, D. Jin, *Nat. Commun.* **2018**, *9*, 2415.

[31] V. T. Vera, D. Mendez-Gonzalez, D. J. Ramos-Ramos, A. Igalla, M. Laurenti, R. Contreras-Caceres, E. Lopez-Cabarcos, E. Díaz, J. Rubio-Retama, S. Melle, O. G. Calderón, *J. Mater. Chem. C* **2021**, *9*, 8902.

[32] H. Fu, C. Hu, J. Liu, Q. Zhang, J. Y. Xu, G. J. Jiang, M. Liu, *CrystEngComm* **2022**, *24*, 7698.

[33] W. Xiao, D. Wu, L. Zhang, X. Zhang, Z. Hao, G.-H. Pan, H. Zhao, L. Zhang, J. Zhang, *J. Phys. Chem. C* **2017**, *121*, 2998.

[34] K. Prorok, M. Olk, M. Skowicki, A. Kowalczyk, A. Kotulska, T. Lipiński, A. Bednarkiewicz, *Nanoscale Adv.* **2019**, *1*, 3463.

[35] G. Sun, Y. Xie, Y. Wang, G. A. Mandl, S. L. Maurizio, H. Zhang, X. Ottenwaelder, J. A. Capobianco, L. Sun, *Angew. Chem., Int. Ed.* **2023**, *62*, 202304591.

[36] D. Zare, Y. Suffren, L. Guénée, S. V. Eliseeva, H. Nozary, L. Aboshyan-Sorgho, S. Petoud, A. Hauser, C. Piguet, *Dalton Trans.* **2015**, *44*, 2529.

[37] L. K. Soro, C. Charpentier, F. Przybilla, Y. Mély, A. M. Nonat, L. J. Charbonnière, *Chemistry* **2021**, *3*, 1037.

[38] S. Petit, F. Baril-Robert, G. Pilet, C. Reber, D. Luneau, *Dalton Trans.* **2009**, *34*, 6809.

[39] D. L. Dexter, J. H. Schulman, *J. Chem. Phys.* **2004**, *22*, 1063.

[40] J. Liu, T. Fu, C. Shi, *J. Phys. Chem. C* **2020**, *124*, 25509.

[41] L. B. Shaw, R. S. F. Chang, N. Djeu, *Phys. Rev. B* **1994**, *50*, 6609.

[42] F. E. Auzel, *Proc. IEEE* **1973**, *61*, 758.

[43] A. I. Burshtein, *J. Lumin.* **1985**, *34*, 167.

[44] A. I. Burshteĭn, *Sov. Phys. Usp.* **1984**, *27*, 579.

[45] M. Inokuti, F. Hirayama, *J. Chem. Phys.* **1965**, *43*, 1978.

[46] T. h. Z Förster, *Ann. Phys.* **1948**, *437*, 55.

[47] T. Kushida, *J. Phys. Soc. Jpn.* **1973**, *34*, 1318.

[48] M. Inokuti, F. Hirayama, *J. Chem. Phys.* **2004**, *43*, 1978.

[49] D. L. Dexter, *J. Chem. Phys.* **2004**, *21*, 836.

[50] P. Vergeer, T. J. H. Vlugt, M. H. F. Kox, M. I. Hertog, J. P. J. M. Eerden, A. Meijerink, *Phys. Rev. B* **2005**, *71*, 014119.

[51] J. Liu, T. Fu, C. Shi, *J. Phys. Chem. C* **2019**, *123*, 9506.

[52] A. Pilch-Wrobel, A. M. Kotulska, S. Lahtinen, T. Soukka, A. Bednarkiewicz, *Small* **2022**, *18*, 2200464.

[53] M. Y. Hossan, A. Hor, Q. Luu, S. J. Smith, P. S. May, M. T. Berry, *J. Phys. Chem. C* **2017**, *121*, 16592.

[54] K. W. Krämer, D. Biner, G. Frei, H. U. Güdel, M. P. Hehlen, S. R. Lüthi, *Chem. Mater.* **2004**, *16*, 1244.

[55] B. Chen, F. Wang, *Acc. Chem. Res.* **2020**, *53*, 358.